ACTA ONCOLOGICA
2021, VOL. 60, NO. 8, 1038–1044
https://doi.org/10.1080/0284186X.2021.1907860

Taylor & Francis
Taylor & Francis Group

ORIGINAL ARTICLE

Cardiac substructure exposure in breast radiotherapy: a comparison between intensity modulated proton therapy and volumetric modulated arc therapy

Pierre Loap, Nicolas Tkatchenko, Farid Goudjil, Madison Ribeiro, Brian Baron, Alain Fourquet and Youlia Kirova

Institut Curie, Department of Radiation Oncology, Paris, France

ABSTRACT

Introduction: Proton therapy for breast cancer treatment reduces cardiac radiation exposure. Left-sided breast cancer patients with indication for internal mammary chain (IMC) irradiation are most at risk of radiation-induced cardiotoxicity. This study aims to evaluate in this situation the potential dosimetric benefit of intensity modulated proton therapy (IMPT) over volumetric modulated arc therapy (VMAT) at the cardiac substructure level.

Materials and methods: Cardiac substructures were retrospectively delineated according to ESTRO guidelines on the simulation CT scans of fourteen left-sided breast cancer patients having undergone conserving surgery and adjuvant locoregional free-breathing (FB-) or deep inspiration breath-hold (DIBH-) VMAT with internal mammary chain irradiation. IMPT treatment was re-planned on the simulation CT scans. Mean doses to cardiac substructures were retrieved and compared between VMAT treatment plans and IMPT simulation plans. Pearson correlation coefficients were calculated between mean doses delivered to cardiac substructures using these two techniques.

Results: Mean doses to all cardiac substructures were significantly lower with IMPT than with VMAT. Regardless of the irradiation technique, the most exposed cardiac substructure was the mid segment of the left anterior descending coronary artery (LADCA). Pearson correlation coefficients between mean doses to cardiac substructures were usually weak and statistically non-significant for IMPT; mean heart dose (MHD) only correlated with mean doses delivered to the right ventricle, to the mid segment of the right coronary artery (RCA) and, to a lesser extent, to the LADCA.

Conclusion: The dosimetric benefit of IMPT over conformal photon therapy was consistently observed for all cardiac substructures. MHD may not be a reliable dosimetric parameter for precise cardiac exposure evaluation when planning IMPT.

ARTICLE HISTORY
Received 5 November 2020
Accepted 19 March 2021

KEYWORDS
Breast cancer; cardiac substructure; intensity modulated proton therapy; intensity modulated radiation therapy

Introduction

Adjuvant radiation therapy for breast cancer treatment improves overall survival after breast conserving surgery [1,2]. However, first generation techniques, which relied on large irradiation fields, were associated with a significantly increased cardiac-related toxicity and mortality [3]. Consequently, technological progresses were made in order to reduce cardiac radiation exposure and state-of-the-art techniques currently allow efficient cardiac sparing, without compromising local tumor control or patient survival. Examples of recent technological breakthroughs for breast cancer treatment include highly conformal photon radiation therapy techniques, such as volumetric modulated arc therapy (VMAT) [4,5], or proton therapy [6]. In addition, these techniques can be efficiently combined with deep inspiration breath-hold (DIBH) in order to further decrease cardiac exposure by mobilizing the heart away from the body surface [7]. Nevertheless, for breast proton therapy, only early and medium-term toxicity profiles are known, due to limited follow-up [8]. Even though short-term tolerance appears excellent [8], long-term cardiotoxicity is still a legitimate matter of concern especially for the youngest patients with internal mammary chain (IMC) irradiation, although long-term analysis of the EORTC 22922/10925 trial is reassuring [9].

In addition, the heart is usually considered as a homogeneous organ-at-risk when planning breast radiotherapy in daily practice since its substructures are usually not delineated nor considered for treatment optimization. Yet, the vast range of potentially lethal radiation-induced cardiac adverse events (such as coronary artery disease, heart failure, pericarditis, arrhythmia or valvular disease, amongst others) is straightforwardly explained by the histological, structural and functional complexity of the heart [10,11]. This is evidenced by recent lung and breast studies that have unambiguously demonstrated that distinctive cardiac adverse events were significantly associated with specific cardiac substructure exposure [12–15]. Considering cardiac substructure exposure during treatment planning could thus be clinically relevant: in particular, in the case where doses to cardiac

CONTACT Pierre Loap pierre.loap@gmail.com Institut Curie, Department of Radiation Oncology, Paris 75248, France
Supplemental data for this article is available online at https://doi.org/10.1080/0284186X.2021.1907860

substructures are poorly correlated and may vary independently, mean heart dose (MHD) would be insufficiently representative to accurately evaluate substructure radiation exposure.

In this context, the goal of this study was to compare at the cardiac substructure level the dosimetric performances of proton therapy and of VMAT, in the adjuvant setting for left-sided breast cancer patients with IMC irradiation indication.

Material and methods

Patient selection

This retrospective single-center dosimetric study was conducted in the Department of Radiation Oncology (Institut Curie, Paris, France). Eligible patients, treated for left-sided breast invasive ductal carcinomas, had all undergone breast conserving surgery and adjuvant locoregional irradiation with normo-fractionated VMAT with or without DIBH. All patients had complex target volumes (IMC irradiation, tumor bed boost) or anatomy (such as pectus excavatum) and, for those patients, adequate target volume coverage with 3 D conformal radiotherapy would have not been possible with respect to institutional organ-at-risk (OAR) dose constraints. Indication for VMAT treatment was based on anatomical and dosimetric considerations and validated by a control quality staff. DIBH was systematically recommended for patients who tolerated it. For all patients, planned target volumes included the whole breast with a boost to the tumor bed, the homolateral axillary, interpectoral, supraclavicular and IMC lymph nodes. Patients with breast implants or treated for recurrent or metastatic breast cancers were excluded. The institutional patient database registered 464 breast cancer patients treated with VMAT with these characteristics until October 2019. Fourteen patients were selected by random sampling stratified on DIBH use, so that seven of them had been treated with free-breathing (FB)-VMAT and the seven others with DIBH-VMAT.

VMAT treatment planning and IMPT re-planning

All patients were immobilized in the same position, supine and both arms above the head. All simulation computed-tomography (CT) scans were acquired with the same parameters (non-contrast and using 3 mm slices) and images were transferred to the Varian Eclipse 8.9 treatment planning system (Varian Medical Systems) for VMAT planning. Simulation CT scans for patients who were treated with DIBH were acquired using the Real-Time Position Management (RPM) Respiratory Gating System (Varian Medical Systems). Clinical target volumes (CTV) consisted of the whole breast, the tumor bed and the homolateral regional lymph nodes (IMC, interpectoral and Berg's level II-III-IV lymph nodes). Tumor bed boost was simultaneously delivered. VMAT treatment schedules were normo-fractionated and delivered the total dose of 63 Gy to the tumor bed, 51.8 Gy to the whole breast and 50.4 Gy to the lymph nodes in 28 fractions. Planned target volumes (PTV) were defined with a 5 mm isotropic expansion margin around CTV. Treatment plans were normalized to mean doses to PTV. A minimum of 95% of the prescribed dose was planned to be delivered to 95% of the PTV and a maximum of 107% of the prescribed dose could be delivered to 2% of the PTV. The heart, the right breast, the lungs, the spinal cord and the esophagus were considered as OAR. Dose constraints to OAR were as follow: mean heart dose < 5 Gy, lung $V_{20Gy} < 25\%$ and $V_{30Gy} < 18\%$, right breast maximum dose < 5 Gy and mean dose < 5 Gy (or $<$1Gy if < 40 years), spinal cord maximum dose < 34 Gy, thyroid mean dose < 30 Gy and $V_{50Gy}<10\%$. Four 230° arcs were planned with 6 MeV photons, a maximum dose rate of 600 MU/min and 4° control point spacing. Target volume coverage and OAR exposure were evaluated based on 3 D dose distribution and dose-volume histograms. Patients who were treated with DIBH were monitored using the Varian RPM system, based on an infrared camera and a reflective box placed on the patient's xyphoid in order to measure his thoracic expansion.

For each patient, pencil-beam scanning (PBS) intensity modulated proton therapy (IMPT) was retrospectively re-planned on the initial simulation FB-CT or DIBH-CT scans on the Varian Eclipse proton treatment planning system by medical physicists kept in ignorance of the initial VMAT treatment plans without aiming at dosimetric superiority concerning cardiac dose. Similarly, the prescription doses were 63 Gy (RBE) to the tumor bed, 51.8 Gy to the whole breast and 50.4 Gy (RBE) to the lymph nodes in 28 fractions. For all patients, treatment was planned on a IBA C230 cyclotron with a nominal proton beam energy of 230 MeV and a 65 mm acrylic range shifter based on a single-field uniform dose method. For each patient, one single enface field with a beam angle of 30° was planned. PTV were defined with a 5 mm isotropic expansion margin around CTV and IMPT treatment plans were normalized to mean doses to PTV. Optimization constraints were similar to those of the VMAT plans.

Cardiac segmentation

Cardiac substructures were subsequently contoured on simulation CT scans, on the Varian Eclipse 8.9 treatment planning system (Varian Medical Systems), according to recent delineation guidelines proposed by the Oxford group and endorsed by the European Society for Radiotherapy and Oncology (ESTRO) [16] in order to ensure homogeneity and reproducibility of the cardiac segmentation process. Delineated cardiac substructures were the whole heart, the four cardiac chambers (the left ventricle (LV), the left auricle, the right ventricle and the right auricle), the five left ventricle walls (anterior, lateral, apical, septal and inferior walls), the left main common artery (LMCA), the left anterior descending coronary artery (LADCA, segmented into its proximal, mid and distal segments), the circumflex artery (CxA, segmented into its proximal and distal segments) and the right coronary artery (RCA, segmented into its proximal, mid, distal and posterior descending segments). Cardiac substructure delineation was validated by an experienced senior radiation oncologist. The

dose-volume histograms were retrieved for each patient from the initial VMAT treatment plan and the corresponding simulated IMPT treatment plan, on the Varian Eclipse treatment planning system in both cases. Mean doses delivered to heart and to all other cardiac substructures were extracted. Figure 1 provides an example of VMAT planning and IMPT re-planning and illustrates cardiac segmentation.

Statistical analysis

Statistical analyses were performed using R 3.6.1 software. Normal distribution hypothesis was verified based on Jarque-Bera test and mean doses between VMAT and IMPT were compared using Student paired test. Pearson correlation coefficients were calculated between MHD and mean doses to all cardiac substructures. A p-value $\leq .05$ was considered statistically significant.

Results

Substructure exposure comparison between VMAT and IMPT

Mean doses to all cardiac substructures were significantly lower with IMPT than with VMAT ($p < .01$, Table 1, Figure 2). Regardless of the considered radiation technique, the most exposed substructure was the mid segment of the LADCA (mean doses: 24.1 Gy, 10.9 Gy, 4.0 Gy and 3.1 Gy for FB-VMAT, DIBH-VMAT, FB-IMPT and DIBH-IMPT treatment plans, respectively). The mean dose to the whole LADCA was less than 2 Gy with DIBH-IMPT (0.3 Gy to the proximal segment, 3.1 Gy to the mid segment and 1.4 Gy to the distal segment). Mean doses to other organs-at-risk (contralateral breast, lungs, esophagus) were lower with IMPT than with VMAT (Supplementary Table 1).

Patients treated with DIBH-VMAT had usually lower cardiac substructure exposure than those treated with FB-VMAT, but no substantial difference was observed after IMPT replanning between the two groups. We observed that mean doses to cardiac substructures were usually lower on FB-IMPT plans than on DIBH-VMAT plans (Table 1, Figure 2).

Dosimetric correlation analysis

Pearson correlation coefficients between mean doses to cardiac substructures were usually weak and often statistically non-significant for IMPT (Figure 3). In particular, MHD correlated only with mean doses to the right ventricle, to the mid segment of the RCA and, to a lesser extent, to the whole LADCA. No statistical correlation was found between MHD and mean doses to the left ventricle or to the ventricle walls, with the exception of the septal wall. MHD did not correlate with mean doses to the LMCA, to the CxA or to the RCA. This sharply contrasted with what was observed for VMAT irradiation, for which Pearson correlation coefficients were greater and more frequently statistically significant.

Discussion

In this single-center retrospective dosimetric study, mean doses delivered to twenty-three cardiac substructures were compared between VMAT and IMPT for left-sided breast cancer patients with IMC irradiation. In order to ensure homogeneous and reproducible cardiac segmentation of the limited-size patient set, which is an inherent limitation of the study, we relied on recent guidelines published by the Oxford Group and endorsed by the ESTRO [16]. For all cardiac substructures, we demonstrated a dosimetric benefit of IMPT over VMAT, which is a highly conformal photon radiation technique. These findings show that the long-recognized cardiac dosimetric benefit of proton therapy for breast cancer [17–22] is consistently found at the lowest level of granularity, whatever cardiac substructure is considered. Doses to the thyroid were similar between IMPT and VMAT plan, which might be explained by its direct proximity with Berg's level IV lymph nodes. A global cardiac dosimetric benefit of proton therapy has similarly been demonstrated for mediastinal lymphoma [23,24], thymic malignancy [25,26], esophageal carcinoma [27,28] and lung cancer [29] irradiation. Although no study has precisely studied cardiac substructure exposure in those situations, one can reasonably infer from our results that this dosimetric benefit would also be found at the cardiac substructure level.

After IMPT replanning, we did not observe notable difference in substructure exposure between free-breathing and DIBH patients; this may question DIBH use for breast IMPT. Published small-size breast proton therapy cohorts did not use DIBH to date [8]. However, our limited number of patients was probably insufficient to evidence any dosimetric benefit of DIBH for IMPT. Nevertheless, it should be recalled that proton therapy is particularly sensitive to uncertainties, such as range or motion uncertainty. DIBH efficiently limits breathing-induced thoracic motion and may consequently avoid potential target under-dosing, which could happen with FB-IMPT. Our IMPT plans were based on a traditional PTV approach, in accordance with our current institutional protontherapy protocols. However, robust optimization method are increasingly used to mitigate the dosimetric effects of patient positioning and proton beam range uncertainties [30,31]. Arm position is another acquisition parameter which should be discussed: it has been shown that arms-down positioning did not affect target coverage nor organ-at-risk exposure compared to standard arms-up positioning [32]. Although the dosimetric equivalence at the cardiac substructure level of arms-up positioning is also logically expected, this is still to be determined.

For IMPT, correlation coefficients between mean doses to the cardiac substructures were globally weak and non-significant, contrasting with what was observed with VMAT. Some negative correlations were unexpectedly observed; this could be explained by statistical fluctuations due to small sample size. It should be stressed that MHD did not correlate with most substructure mean doses. Consequently, MHD should not be considered as a reliable surrogate dosimetric parameter for precise evaluation of cardiac substructure exposure when planning IMPT. Implications are clinically far-reaching:

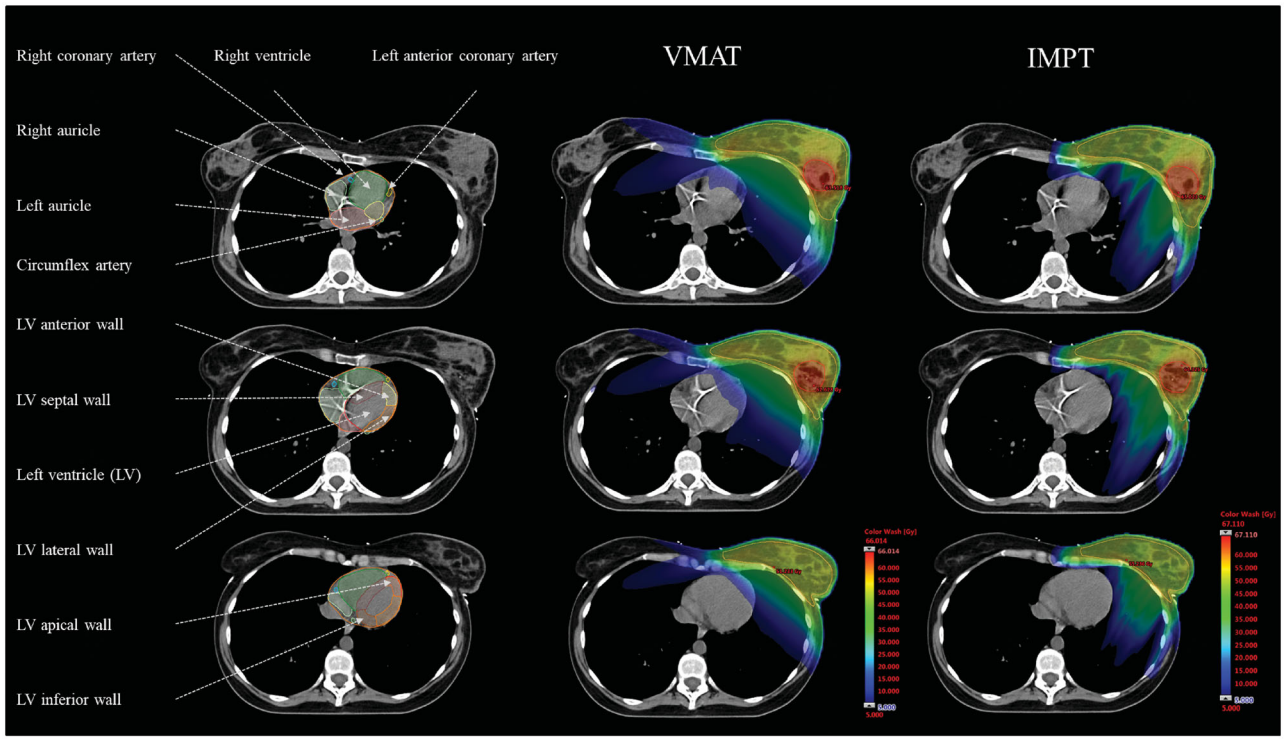

Figure 1. Example of VMAT planning and IMPT re-planning. Cardiac substructures were delineated on the initial simulation CT scans according to ESTRO guidelines. The tumor bed is delineated in red and the left breast in yellow. The internal mammary chain is delineated in cyan. LV: left ventricle.

Table 1. Comparison between mean doses to cardiac substructures using volumetric modulated arc therapy (VMAT) and intensity modulated proton therapy (IMPT).

	FB ($n=7$) + DIBH ($n=7$)			FB ($n=7$)			DIBH ($n=7$)		
Structure	VMAT	IMPT	*p* value	VMAT	IMPT	*p* value	VMAT	IMPT	*p* value
Heart	5.01	0.52	<.01	7.12	0.80	<.01	3.50	0.32	<.01
Left ventricle	4.95	0.16	<.01	7.40	0.09	<.01	3.19	0.22	<.01
Anterior wall	8.24	0.53	<.01	12.47	0.26	<.01	5.23	0.72	<.01
Apical wall	7.72	0.68	<.01	12.38	0.40	<.01	4.39	0.88	<.01
Lateral wall	4.72	0.11	<.01	6.60	0.04	<.01	3.37	0.16	<.01
Inferior wall	2.69	<0.01	<.01	4.13	<0.01	<.01	1.65	0.01	<.01
Septal wall	4.38	0.02	<.01	6.62	0.02	<.01	2.77	0.01	<.01
Right ventricle	5.01	0.37	<.01	7.05	0.79	<.01	3.55	0.07	<.01
Left auricle	2.77	<0.01	<.01	3.97	<0.01	<.01	1.91	<0.01	<.01
Right auricle	3.05	0.04	<.01	3.89	0.06	<.01	2.44	0.03	<.01
Left main coronary artery	4.30	0.01	<.01	6.34	0.02	<.01	2.85	<0.01	<.01
Left anterior descending artery	13.69	1.99	<.01	21.19	2.48	<.01	8.32	1.65	.01
Proximal segment	8.43	0.25	<.01	12.99	0.19	.01	5.17	0.29	<.01
Mid segment	16.39	3.49	<.01	24.10	4.00	<.01	10.88	3.13	.02
Distal segment	14.68	1.70	<.01	23.52	2.15	.01	8.37	1.38	.01
Circumflex artery	3.62	<0.01	<.01	5.12	<0.01	<.01	2.54	<0.01	<.01
Proximal segment	4.86	<0.01	<.01	7.34	<0.01	<.01	3.09	0.01	<.01
Distal segment	3.30	<0.01	<.01	4.53	<0.01	<.01	2.41	<0.01	<.01
Right coronary artery	3.92	0.05	<.01	5.40	0.03	<.01	2.87	0.06	<.01
Proximal segment	5.36	0.11	<.01	6.45	0.06	<.01	4.58	0.14	.01
Mid segment	3.06	<0.01	<.01	4.15	0.01	<.01	2.27	<0.01	<.01
Distal segment	1.93	<0.01	<.01	3.01	<0.01	<.01	1.17	<0.01	<.01
Posterior descending segment	3.48	<0.01	<.01	6.15	<0.01	<.01	1.56	<0.01	<.01
Left lung	13.53	8.38	<.01	15.24	6.83	<.01	12.3	9.49	.02
Right lung	4.39	0.70	<.01	5.48	1.13	<.01	3.61	0.4	<.01

Comparison were carried out in the overall population ($n=14$), in the free-breathing (FB) subpopulation ($n=7$) and in the DIBH population ($n=7$), using Student paired t-tests.

to have a clear picture of cardiac exposure when planning proton therapy, one would have to consider and to delineate all cardiac substructures. For VMAT, MHD correlated significantly with most cardiac substructures but poorly with the RCA, the LADCA (distal segment) and the LV (apical wall) which delineations could be considered in clinical practice [33]. Currently, substructure dose constraints are mostly unknown for photon or proton therapy, and their estimation

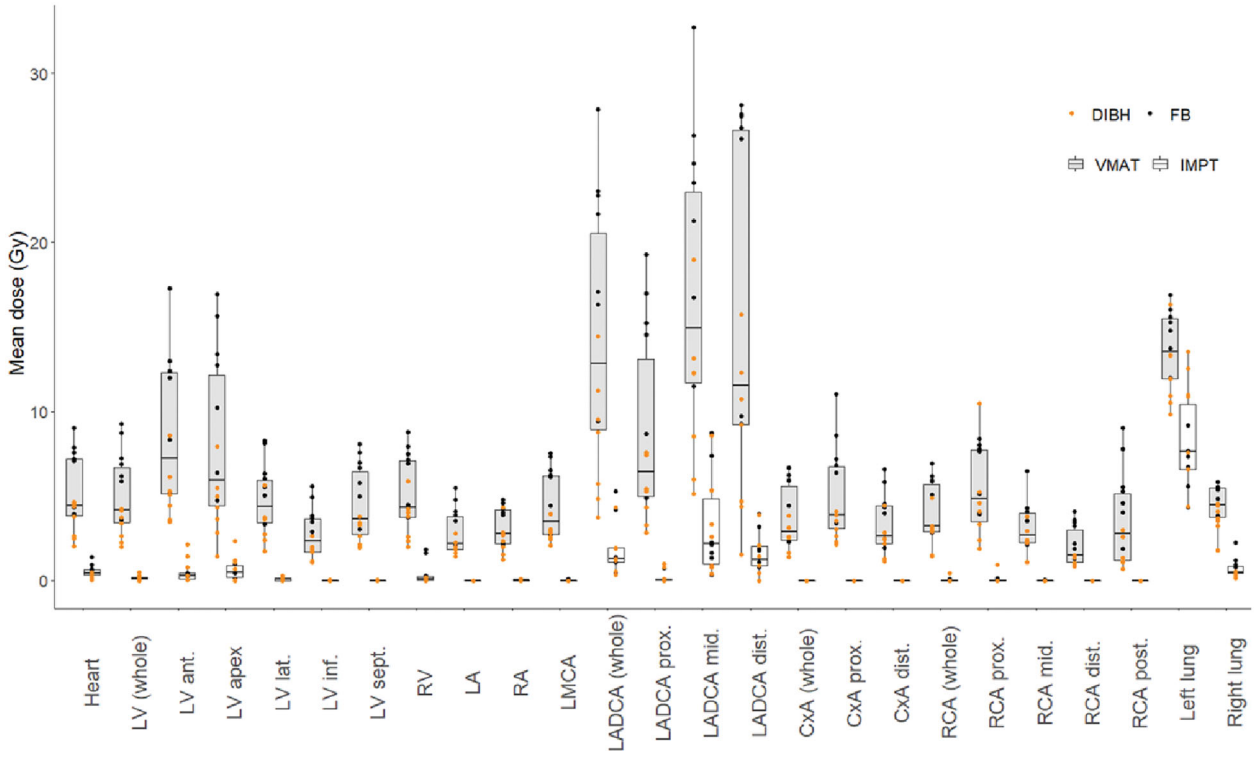

Figure 2. Boxplot distributions of mean doses to cardiac substructures. Boxplots provide the median, the quartiles and the range of mean dose distributions for each cardiac substructure. LV: left ventricle. RV: right ventricle. LA: left auricle. RA: right auricle. LV ant: LV anterior wall. LV apex: LV apical wall. LV lat: LV lateral wall. LV inf: LV inferior wall. LV sept: LV septal wall LMCA: left main coronary artery. LADCA: left anterior descending coronary artery. CxA: circumflex artery. RCA: right coronary artery. DIBH: deep inspiration breath-hold. FB: free breathing. VMAT: volumetric modulated arc therapy. IMPT: intensity modulated proton therapy. Orange dots correspond to DIBH treatments, black dots to FB treatments.

will take time [34]. Yet, propositions already exist for the left ventricle and for the left anterior descending artery [33,35]. The increasing interest for breast proton therapy and the subsequent multiplication of long-term prospective cohorts may help clarifying substructure dose constraints over the long term, once cardiac segmentation is widely implemented in clinical research and daily practice. Since recent photon radiation therapy trials focusing on lung and breast cancers have demonstrated that different types of cardiac adverse events were associated with specific cardiac substructure exposure [12–15], it would be logically expected that this may also be the case for proton therapy and, in this context, breast proton therapy planning will have to consider cardiac segmentation.

Delineation of cardiac substructure is time-consuming when manually done, and non-contrast simulation CT scans are often imprecise for precise cardiac segmentation. Fortunately, recent auto-segmentation algorithms, either atlas-based [36–41] or deep-learning-based [42–44], have already shown promising results. It is highly expected that, in the near future, reliable artificial intelligence tools could be routinely used for cardiac auto-segmentation, both for clinical research and in daily practice. With this in mind, radiation oncologist should collaborate with medical artificial intelligence experts in order to develop trustworthy and ergonomic auto-segmentation softwares.

Even though long-term analysis of the EORTC 22922/10925 trial did not find any increase in cardiovascular risk associated with IMC irradiation [9], left-sided breast cancer patients with IMC irradiation indication are theoretically the most at risk of developing late radiation-induced cardiotoxicity risk, in particular the youngest patients which have logically the highest lifetime cumulative risk. This clinical presentation represents a relatively small proportion of all breast cancer patients; however, in this situation, proton therapy demonstrates a substantial dosimetric benefit over photon therapy, even when this latter is combined with DIBH, which is already routinely the case in such circumstances. Long-term cardiotoxicity studies are needed to confirm that this dosimetric superiority clinically translates into fewer radiation-induced cardiac adverse events or deaths in such contexts. The RadComp randomized controlled trial (NCT02603341), comparing proton versus photon radiation therapy on a cardiotoxicity primary criterion, will provide elements to answer this question [45]. In the meantime, dosimetric criteria should be established in order to select the best candidates for breast IMPT.

In conclusion, taking into account ESTRO guidelines for cardiac segmentation, we demonstrated that the dosimetric benefit of IMPT over conformal photon therapy was consistently observed for all cardiac substructures. MHD may not be a reliable dosimetric parameter for precise cardiac exposure evaluation for breast IMPT and it may not accurately reflect long-term cardiotoxicity with this technique if it eventually appears that cardiac adverse events are correlated with specific substructure exposure. Long-term breast cancer

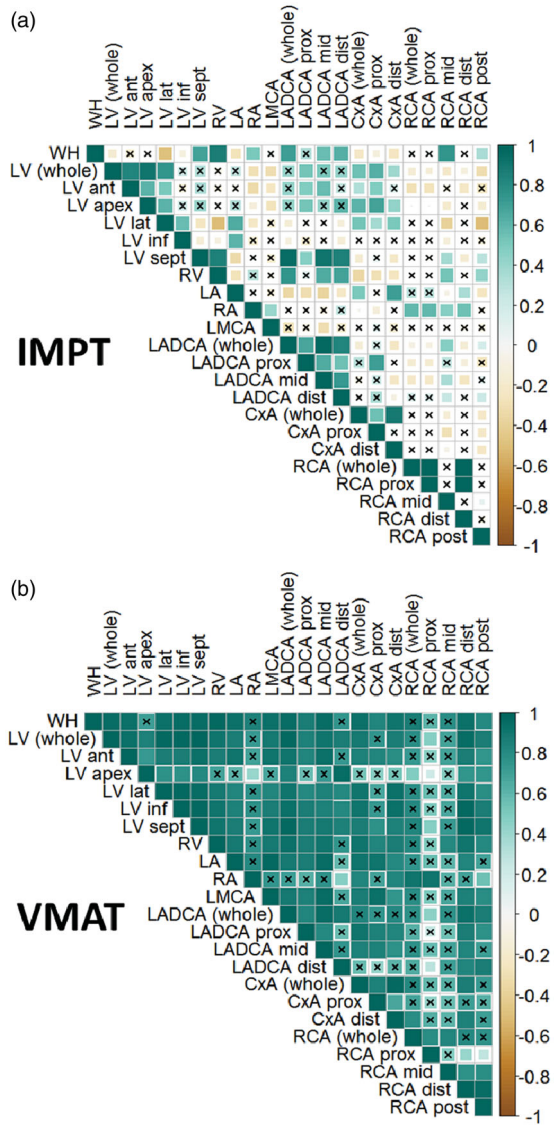

Figure 3. Correlation matrices between mean doses to cardiac substructures for intensity modulated proton therapy (IMPT, a.) and volumetric modulated arc therapy (VMAT, b). Correlation strength (r value) is indicated by the color of the box (ranging between −1 and 1). A crossed box refers to a non-significant correlation. LV: left ventricle. LA: left auricle. RV: right ventricle. RA: right auricle. LMCA: left main coronary artery. LADCA: left anterior descending coronary artery. CxA: circumflex artery. RCA: right coronary artery.

proton therapy studies are needed to evaluate late cardiotoxicity and to define specific cardiac substructure dose constraints.

Data sharing

Research data are stored in an institutional repository and will be shared upon request to the corresponding author.

Disclosure statement

No potential conflict of interest was reported by the author(s).

ORCID

Pierre Loap http://orcid.org/0000-0001-8863-8110

References

[1] Clarke M, Collins R, Darby S, et al. Effects of radiotherapy and of differences in the extent of surgery for early breast cancer on local recurrence and 15-year survival: an overview of the randomised trials. Lancet Lond Engl. 2005;366:2087–2106.

[2] , McGale P, Taylor C, EBCTCG (Early Breast Cancer Trialists' Collaborative Group), et al. Effect of radiotherapy after mastectomy and axillary surgery on 10-year recurrence and 20-year breast cancer mortality: meta-analysis of individual patient data for 8135 women in 22 randomised trials. Lancet Lond Engl. 2014; 383:2127–2135.

[3] Darby SC, Ewertz M, McGale P, et al. Risk of ischemic heart disease in women after radiotherapy for breast cancer. N Engl J Med. 2013;368(11):987–998.

[4] Lauche O, Kirova YM, Fenoglietto P, et al. Helical tomotherapy and volumetric modulated arc therapy: new therapeutic arms in the breast cancer radiotherapy. World J Radiol. 2016;8(8):735–742.

[5] Loap P, Fourquet A, Kirova Y. The Limits of the Linear Quadratic (LQ) model for late cardiotoxicity prediction: example of hypofractionated rotational Intensity Modulated Radiation Therapy (IMRT) for breast cancer. Int J Radiat Oncol Biol Phys. 2020;106(5): 1106–1108.

[6] Fagundes M, Hug EB, Pankuch M, et al. Proton therapy for locally-regionally advanced breast cancer maximizes cardiac sparing. Int J Part Ther. 2015;1(4):827–844.

[7] Bergom C, Currey A, Desai N, et al. Deep inspiration breath hold: techniques and advantages for cardiac sparing during breast cancer irradiation. Front Oncol. 2018;8:87. https://www.ncbi.nlm.nih.gov/pmc/articles/PMC5893752/.

[8] Jimenez RB, Hickey S, DePauw N, et al. Phase II study of proton beam radiation therapy for patients with breast cancer requiring regional nodal irradiation. J Clin Oncol. 2019;37(30):2778–2785.

[9] Poortmans PM, Weltens C, Fortpied C, et al. Internal mammary and medial supraclavicular lymph node chain irradiation in stage I–III breast cancer (EORTC 22922/10925): 15-year results of a randomised, phase 3 trial. Lancet Oncol. 2020;21(12):1602–1610.

[10] Mery B, Guichard J-B, Guy J-B, et al. Atrial fibrillation in cancer patients: hindsight, insight and foresight. Int J Cardiol. 2017;240: 196–202.

[11] Taunk NK, Haffty BG, Kostis JB, et al. Radiation-induced heart disease: pathologic abnormalities and putative mechanisms. Front Oncol. 2015;5:39. https://www.ncbi.nlm.nih.gov/pmc/articles/PMC4332338/.

[12] Reshko LB, Kalman NS, Hugo GD, et al. Cardiac radiation dose distribution, cardiac events and mortality in early-stage lung cancer treated with stereotactic body radiation therapy (SBRT). J Thorac Dis. 2018;10(4):2346–2356.

[13] Stam B, Peulen H, Guckenberger M, et al. Dose to heart substructures is associated with non-cancer death after SBRT in stage I-II NSCLC patients. Radiother Oncol. 2017;123(3):370–375.

[14] Chen VE, Song AJ, Werner-Wasik M, et al. Effect of radiation dose to cardiac substructures on the acute development of new arrhythmias following conventionally fractionated radiation treatment to the lung. Int J Radiat Oncol Biol Phys. 2019;105(1):E500.

[15] Early detection of subclinical left ventricular dysfunction after breast cancer radiation therapy using speckle-tracking echocardiography: association between cardiac exposure and longitudinal strain reduction (BACCARAT study). – Abstract – Europe PMC [Internet]; [cited 2020 Jan 28]. Available from: https://europepmc.org/article/PMC/6854785.

[16] Duane F, Aznar MC, Bartlett F, et al. A cardiac contouring atlas for radiotherapy. Radiother Oncol. 2017;122(3):416–422.

[17] Hernandez M, Zhang R, Sanders M, et al. A treatment planning comparison of volumetric modulated arc therapy and proton

therapy for a sample of breast cancer patients treated with postmastectomy radiotherapy. J Proton Ther. 2015;1:119.
[18] Sun T, Lin X, Tong Y, et al. Heart and cardiac substructure dose sparing in synchronous bilateral breast radiotherapy: a dosimetric study of proton and photon radiation therapy. Front Oncol. 2019; 9:1456.
[19] Jimenez RB, Goma C, Nyamwanda J, et al. Intensity modulated proton therapy for postmastectomy radiation of bilateral implant reconstructed breasts: a treatment planning study. Radiother Oncol. 2013;107(2):213–217.
[20] Ares C, Khan S, Macartain AM, et al. Postoperative proton radiotherapy for localized and locoregional breast cancer: potential for clinically relevant improvements? Int J Radiat Oncol Biol Phys. 2010;76(3):685–697.
[21] Weber DC, Ares C, Lomax AJ, et al. Radiation therapy planning with photons and protons for early and advanced breast cancer: an overview. Radiat Oncol. 2006;1:22.
[22] Mast ME, Vredeveld EJ, Credoe HM, et al. Whole breast proton irradiation for maximal reduction of heart dose in breast cancer patients. Breast Cancer Res Treat. 2014;148(1):33–39.
[23] Ricardi U, Maraldo MV, Levis M, et al. Proton therapy for lymphomas: current state of the art. Onco Targets Ther. 2019;12: 8033–8046.
[24] Abbassi LM, Goudjil F, Arsène-Henry A, et al. Protontherapy versus best photon for mediastinal Hodgkin lymphoma: dosimetry comparison and treatment using ILROG guidelines. Cancer Radiother. 2019;23(8):922–925.
[25] Parikh RR, Rhome R, Hug E, et al. Adjuvant proton beam therapy in the management of thymoma: a dosimetric comparison and acute toxicities. Clin Lung Cancer. 2016;17(5):362–366.
[26] Zhu HJ, Hoppe BS, Flampouri S, et al. Rationale and early outcomes for the management of thymoma with proton therapy. Transl Lung Cancer Res. 2018;7(2):106–113.
[27] Xi M, Xu C, Liao Z, et al. Comparative outcomes after definitive chemoradiotherapy using proton beam therapy versus intensity modulated radiation therapy for esophageal cancer: a retrospective, single-institutional analysis. Int J Radiat Oncol Biol Phys. 2017;99(3):667–676.
[28] Lin SH, Hobbs BP, Verma V, et al. Randomized phase IIB trial of proton beam therapy versus intensity-modulated radiation therapy for locally advanced esophageal cancer. J Clin Oncol off J Am Soc Clin Oncol. 2020;38(14):1569–1579.
[29] Gjyshi O, Liao Z. Proton therapy for locally advanced non-small cell lung cancer. Br J Radiol. 2020;93(1107):20190378.
[30] Korevaar EW, Habraken SJM, Scandurra D, et al. Practical robustness evaluation in radiotherapy – a photon and proton-proof alternative to PTV-based plan evaluation. Radiother Oncol. 2019; 141:267–274.
[31] Ranger A, Dunlop A, Hutchinson K, et al. A dosimetric comparison of breast radiotherapy techniques to treat locoregional lymph nodes including the internal mammary Chain. Clin Oncol R Coll Radiol G B. 2018;30(6):346–353.
[32] Batin E, Depauw N, MacDonald S, et al. EP-2084 Arms-down versus arms-up positioning for breast cancer patients receiving proton beam radiation. Radiother Oncol. 2019;133:S1150–S1151.
[33] Piroth MD, Baumann R, Budach W, et al. Heart toxicity from breast cancer radiotherapy: current findings, assessment, and prevention. Strahlenther Onkol. 2019;195(1):1–12.
[34] Loap P, Fourquet A, Kirova Y. Should we move beyond mean heart dose? Int J Radiat Oncol Biol Phys. 2020;107(2):386–387.
[35] van den Bogaard VAB, van Luijk P, Hummel YM, et al. Cardiac function after radiation therapy for breast cancer. Int J Radiat Oncol Biol Phys. 2019;104(2):392–400.
[36] Zhou R, Liao Z, Pan T, et al. Cardiac atlas development and validation for automatic segmentation of cardiac substructures. Radiother Oncol. 2017;122(1):66–71.
[37] Shahzad R, Bos D, Budde RPJ, et al. Automatic segmentation and quantification of the cardiac structures from non-contrast-enhanced cardiac CT scans. Phys Med Biol. 2017;62(9):3798–3813.
[38] Luo Y, Xu Y, Liao Z, et al. Automatic segmentation of cardiac substructures from noncontrast CT images: accurate enough for dosimetric analysis? Acta Oncol Stockh Swed. 2019;58(1):81–87.
[39] Jung JW, Lee C, Mosher EG, et al. Automatic segmentation of cardiac structures for breast cancer radiotherapy. Phys Imaging Radiat Oncol. 2019;12:44–48.
[40] Maffei N, Fiorini L, Aluisio G, et al. Hierarchical clustering applied to automatic atlas based segmentation of 25 cardiac sub-structures. Phys Med. 2020;69:70–80.
[41] Finnegan R, Dowling J, Koh E-S, et al. Feasibility of multi-atlas cardiac segmentation from thoracic planning CT in a probabilistic framework. Phys Med Biol. 2019;64(8):085006.
[42] Morris ED, Ghanem AI, Dong M, et al. Cardiac substructure segmentation with deep learning for improved cardiac sparing. Med Phys. 2020;47(2):576–586.
[43] Zhuang X, Li L, Payer C, et al. Evaluation of algorithms for multi-modality whole heart segmentation: an open-access grand challenge. ArXiv190207880 Cs [Internet]. 2019; [cited 2020 Mar 15]. Available from: http://arxiv.org/abs/1902.07880.
[44] Chen C, Qin C, Qiu H, et al. Deep learning for cardiac image segmentation: a review. Front Cardiovasc Med. 2020;7:25. https://www.frontiersin.org/articles/10.3389/fcvm.2020.00025/full.
[45] Bekelman JE, Lu H, Pugh S, et al. Pragmatic randomised clinical trial of proton versus photon therapy for patients with non-metastatic breast cancer: the Radiotherapy Comparative Effectiveness (RadComp) Consortium trial protocol. BMJ Open. 2019;9(10): e025556.